How ubiquitous is the dipole relationship in tropical Atlantic sea surface temperatures?

David B. Enfield [1], Alberto M. Mestas-Nuñez [2], Dennis A. Mayer [1], and Luis Cid-Serrano [3]

[1] NOAA Atlantic Oceanographic and Meteorological Laboratory

4301 Rickenbacker Cswy, Miami, FL 33149 USA

[2] Cooperative Institute for Marine and Atmospheric Studies

4600 Rickenbacker Cswy, Miami, FL 33149 USA

[3] Statistics Department, University of Concepción

Concepción, Chile

Resubmitted to

Journal of Geophysical Research

November 1998

Abstract. Several kinds of analysis are applied to the departures of sea surface temperatures from climatology (SSTA, 1856-1991) to determine the degree to which SSTA of opposite sign in the tropical North and South Atlantic occur. Antisymmetric ("dipole") configurations of SSTA on basin scales are not ubiquitous in the tropical Atlantic. Unless the data are stratified by both season and frequency, inherent dipole behavior cannot be demonstrated. Upon removing the global ENSO signal in SSTA (which is symmetric between the North and South Atlantic) from the data, the regions north or south of the intertropical convergence zone have qualitatively different temporal variabilities and are poorly correlated. Dipole configurations do occur infrequently (12-15% of the time), but no more so than expected by chance for stochastically independent variables. Non-dipole configurations that imply significant meridional SSTA gradients occur much more frequently, nearly half of the time. Cross-spectral analysis of seasonally averaged SSTA indices for the North and South Atlantic show marginally significant coherence with antisymmetric phase in two period bands: 8-12 years for the boreal winter-spring, and 2.3 years for the boreal summer-fall. Antisymmetric coherence is optimal for a small sub-region west of Angola in the South Atlantic, with respect to SSTA of basin scale in the tropical North Atlantic. Dipole variability, even where optimal, explains only a small fraction of the total variance in tropical Atlantic SSTA (< 7%).

1. Introduction

Starting in the 1970s, many examples have been given of the relevance to tropical Atlantic climate variability of meridionally antisymmetric (opposite sign) distributions of sea surface temperature anomaly (SSTA) and associated sea level pressure anomaly (SLPA) across the Atlantic intertropical convergence zone (ITCZ) [*Hastenrath*, 1976; *Moura and Shukla*, 1981; *Folland et al.,* 1986; *Lamb and Peppler*, 1992; *Hastenrath and Greischar*, 1993; *Nobre and Shukla*, 1996]. Manifestations of such "dipole" variability in SSTA have been obtained from empirical orthogonal function (EOF) analyses and have led to the proposal of a dipole index of SSTA based on the difference between area indices of SSTA north and south of the ITCZ [*Weare*, 1977; *Servain*, 1991]. More recently, *Carton et al.* [1996] and *Chang et al.* [1997] have proposed a plausible mechanism to explain how variability of the meridional SSTA gradient can result from tropical ocean-atmosphere interactions. A singular value decomposition (SVD) of SSTA and wind stress is consistent with such a mechanism and the dominant regression pattern for SSTA is dipole-like [*Chang et al.* 1997]. The authors make it clear, however, that their model results are more significant as a mechanism for generating meridional gradient variability than as a justification for a dipole relationship.

Other studies, while not denying the relevance of antisymmetric SSTA configurations to climate variability, have questioned the notion that dipole variability occurs as an intrinsic mode of fluctuation in Atlantic SSTA. As in *Weare* [1977], *Houghton and Tourre* [1992] find a dipole structure in the second mode of an EOF analysis. However, the decomposition is unstable, as evidenced by poor separation between the first and second eigenvalues. The local explained variance over the northern and southern regions of such antisymmetric modes is significant but not very high. Upon performing a varimax rotation of the ordinary EOF modes, the decomposition stabilizes into regionalized modes with well separated eigenvalues. Each rotated mode has high local explained variance on one side or the other of the ITCZ

[*Houghton and Tourre*, 1992]. For different space-time domains and without the need for varimax rotation, *Enfield and Mayer* [1997] extract stable modes with separated eigenvalues and high explained variance both south (first mode) and north (second mode) of the ITCZ. They find insignificant correlations between the northern and southern modes out to lags greater than one year. *Enfield* [1996] represents the tropical SSTA variability with two simple area indices north and south of the ITCZ. The indices are highly correlated with the respective EOF modes of *Enfield and Mayer* [1997] but are not significantly correlated with each other. *Rajagopalan et al.* [1998] find that this lack of correlation applies at all time scales. Finally, *Mehta* [1998] shows that decadal and longer variations in a dipole SSTA index (north minus south) are really a reflection of meridional gradient variability and that no dynamical-thermodynamical dipole mode exists for SSTA during his analysis period.

The latter studies suggest that an intrinsic dipole mode of SSTA variability does not exist, although dipole configurations may occur randomly and still enhance climate anomalies over the tropical Atlantic and surrounding land regions. However, no study heretofore has unequivocally resolved the question of dipole variability for several reasons. First, the temporal domain of most studies has been limited to the recent decades of the twentieth century in which decadal and longer time scales are sometimes diminished by trend removal, are not well-resolved statistically, and are superimposed on strong interannual SSTA variability. Although *Mehta's* [1998] more recent work stands as a clarification, *Mehta and Delworth* [1995] find indications that dipole variability may indeed be weak or absent in data sets dominated by interannual frequencies [e.g., *Enfield and Mayer*, 1997], yet more significant at decadal or longer time scales. Second, there is the possibility that interannual variability connected with the Pacific El Niño-Southern Oscillation (ENSO) [*Enfield and Mayer*, 1997], which is mainly symmetric across the ITCZ, masks

any tendency for antisymmetric behavior. Finally, previous studies do not distinguish between seasons.

In this paper, we seek to clarify the confusing and apparently contradictory views regarding tropical Atlantic dipole variability. The issue is revisited by using a recently reconstructed, 136-year SSTA analysis for the globe [*Kaplan et al*., 1998; henceforth, K98]. In section 3 we address the complication of connected ENSO variability with a rotated EOF analysis of SSTA in which a global ENSO mode is first removed from the data; see *Enfield and Mestas-Nuñez* [1998]. We then probe the question of dipole ubiquity directly with a probability analysis of alternate basin configurations (section 4). Finally, (section 5), the coherence and phase between regions north and south of the ITCZ is then examined using crosscorrelation and cross-spectral analyses of seasonally averaged area indices of SSTA. In section 6 we discuss the significance of the results and what it means for climate research questions posed in the future.

2. Data and methods

The issue in question is only the degree of antisymmetric association between SSTA north and south of the ITCZ and not the relationships between SSTA and other climate variables. Hence, the only data used in this study are the K98 data for global SSTA, with trends removed everywhere. These data are monthly on a global 5°x5° grid and span the period 1856-1991. The K98 analysis method optimizes a least-squares cost function to recover large-scale SSTA patterns during earlier periods of sparse sampling. *Kaplan et al*. [1998] compare their SSTA analysis to other cost-function optimization methods and to the Global Ocean Surface Temperature Atlas (GOSTA) [*Bottomley et al*., 1990]. They find their analysis most similar to those of *Smith et al*. [1996] and *Shriver and O'Brien* [1995], with very little difference between methods during modern times (e.g., after 1950). Although analysis errors increase notably in the Pacific prior to about 1880, the authors find the

analyzed Pacific data useful as far back as the 1860s. The century scale K98 data set is especially useful for looking at basin-scale relationships such as applies herein. Moreover, they can resolve a wide range of frequencies and can account for the Pacific ENSO and its teleconnections to other ocean basins.

We split the analysis into several phases. To begin with (section 3), we show how Atlantic SSTA decomposes in a rotated EOF (REOF) analysis of the K98 data after first removing global ENSO variability. For the REOF analysis, we remove annual and higher frequencies with a quadratic Loess smoother having a half-span of 1.5 years. The global ENSO variability is captured by the leading mode of a complex EOF analysis of bandpassed SSTA (1.5-8 years) [*Enfield and Mestas-Nuñez*, 1998]. By focusing on the structure of the non-ENSO residuals, we minimize the symmetric ENSO response that may mask antisymmetric, non-ENSO variability at interannual frequencies. All other variability, at periodicities from 2 years to multidecadal, is retained in the residual data.

In a second analysis (section 4) we examine the frequency of occurrence of simple area indices north and south of the ITCZ, for the sub-domains of a contingency table. This enables us to assess the ubiquity of dipole configurations, compare it with that expected by chance, and contrast it with the much greater frequency of non-dipole, meridional gradients.

Subsequently (section 5), we use crosscorrelation and cross-spectral analyses of the K98 data to test the null hypothesis that area indices of SSTA north and south of the ITCZ are unrelated to each other (no dipole). To account for seasonal differences and intraseasonal variability we do not use a smoothed version of the data; we perform analyses of the unsmoothed data with and without the global ENSO mode removed.

We define a tropical North Atlantic (TNA) index to be the average of the monthly data over the rectangular region 5°N-25°N, 55°W-15°W. The tropical

South Atlantic (TSA) index is the average over a region of equal area, 20°S-0°, 30°W-10°E. These index domains (see Fig. 1) are consistent with the EOF decomposition of *Enfield and Mayer* [1997] and correspond approximately to the recommendations of *Servain* [1991]. Based on indications from the REOF analysis, we also define an area index over a 10° square straddling the Greenwich meridian west of Angola (5°W-5°E, 10°S-20°S). We denote this index as TSA-2.

3. Non-ENSO variability in the Atlantic

Enfield and Mestas-Nuñez [1998] represent canonical ENSO variability in the World Ocean by the leading empirical function of a complex EOF analysis of bandpassed (1.5-8 years) K98 data. This permits the extraction – in a single global mode – of ENSO variability complete with its intra-Pacific and other-basin lags of up to three seasons. Tropical Atlantic variability correlates positively in both hemispheres with the Pacific ENSO at lags of one to three seasons. In their analysis of the third ordinary (not complex) EOF mode of the non-ENSO residuals, they find that variabilities in the eastern equatorial Pacific and the tropical South Atlantic are included with variability in the North Atlantic. However, when the EOF decomposition is subjected to a varimax rotation, these three regions separate cleanly into three distinct REOF modes [*Mestas-Nuñez and Enfield*, 1998]. The respective REOF spatial patterns in the tropical North and South Atlantic indicate greater explained variance in those regions than for the single unrotated EOF mode. This is consistent with *Houghton and Tourre* [1992] who use a data set of much smaller temporal extent over only the tropical Atlantic.

So as not to prejudice the possibility of temporal relationships between modes (such as the Atlantic dipole) *Mestas-Nuñez and Enfield* [1998] relax the constraint of temporal orthogonality. This means that the REOFs are spatially orthogonal but the temporal expansion coefficients of the modes may have nonzero correlation. Their study does obtain, for example, significant

contemporaneous correlations between REOF modes having large explained variance in the Pacific. The REOF modes for the North and South Atlantic, however, have only a very small temporal correlation. This is especially significant in view of the fact that global ENSO variability was first removed from the data. Since the ENSO manifestation in the tropical Atlantic is of the same sign on both sides of the equator [*Enfield and Mayer*, 1997], it might otherwise obscure an antisymmetric relationship.

In Fig. 1 we show the spatial distributions (upper panels) for the correlation of the smoothed, residual K98 data with the Atlantic REOF modal reconstructions of SSTA (lower panels) averaged over the north and south index regions (dashed rectangles). The latter are area averages of reconstructions (temperature units) derived from the modal expansion coefficients, rather than of data. As such, we refer to them as NA and SA to distinguish them from the data-derived averages (TNA and TSA) that are used in the next section. Correlations in the range of 0.24-0.28 (0.21-0.24) correspond to the average 95% (90%) significance level after accounting for serial correlation in the data [*Davis*, 1976]. Local correlations within the respective index areas average 0.75 (NA) and 0.8 (SA). In the SA mode, correlations in the NA region are negligible, hence the null hypothesis cannot be rejected anywhere in the North Atlantic with respect to basin-scale fluctuations in the South Atlantic. In other words, basin-scale anomalies in the tropical South Atlantic are not statistically associated with any response in the tropical North Atlantic. In the NA mode there are marginally significant negative correlations at three grid points in a small region west of Angola (dashed contour). Hence, we can only reject the null hypothesis over a small portion of the tropical South Atlantic where there is a very weak tendency for antisymmetry with respect to basin-scale fluctuations in the tropical North Atlantic. We note, however, that only about 7% of the variance is explained by NA over that small region. We will see evidence of this relationship again in the seasonally stratified cross-spectral analysis of the next section. That

analysis includes consideration of the reduced-area index in the South Atlantic (TSA-2).

The temporal reconstructions for NA and SA (Fig. 1, bottom panels) reveal a very different character for the two regions. Both series contain a wide range of frequencies from interannual to multidecadal but the visual appearance of the two is quite distinct. NA has a more multidecadal character than SA, which is more decadal and interannual. The correlation magnitude between the NA and SA time series is less than 0.05 at all lags out to more than a year. Hence, basin-scale fluctuations in the tropical North and South Atlantic appear to be unrelated. The visual appearance of the time series is consistent with the low correlation. We see some periods in which the two regions are clearly antisymmetric (e.g., the 1950s). However, for many other periods NA and SA are of the same sign (e.g., the decade from 1903 to 1912) or of indeterminate relationship (large departures for one or the other but not both).

4. Probability analysis

We now address the issue of ubiquity with a straightforward probability analysis. This is based on a contingency table of occurrence frequencies for which the TNA and TSA indices fall into their respective quartile extreme ranges ($|SSTA| \geq Tq$) or into their bi-quartile mid-range ($|SSTA| < Tq$). The standard deviations are 0.35 °C and 0.34 °C for TNA and TSA, and the inter-quartile threshold (averaged for both) is $Tq = 0.24$ °C. The frequencies of occurrence expressed as fractions of one are shown in Table 1. Using this quartile threshold to define the significant departures of the indices, we see that positive dipole configurations (north positive, south negative) occur 5.9% of the time (lower left cell) and negative dipoles 6.2% of the time (upper right) for a total of 12.1%. If we use a lower threshold of 0.2 °C (not shown), the total dipole frequency rises to 15.4%. Thus, for thresholds within a

reasonable range of values, large-scale dipole configurations occur 12-15% of the time and are therefore not ubiquitous.

How do these dipole frequencies compare to what would be expected purely by chance?. TNA and TSA are uncorrelated (r = 0.05) and a goodness-of-fit test shows that TNA and TSA are normally distributed (p-value=.727 for TNA and .2099 for TSA). With these characteristics they may be considered stochastically independent, random variables [*Bartoszynski and Niewiadomska-Bugag*, 1996]. By a fundamental theorem of statistics [*Hogg and Craig*, 1965] the joint probability distribution for stochastically independent random variables [X,Y] satisfies the relation

$$P(X=x,Y=y) = P(X=x) \bullet P(Y=y)$$

where P denotes probability of occurrence and [x, y] are value domains, such as $|T| \geq Tq$ in the case we are considering. The value ranges for significant departures correspond to the first and third columns (TNA) and rows (TSA) of the contingency matrix and their probabilities are the sums of the same columns and rows. Finally, we see that the expected total occurrence frequency for dipole configurations is simply $(0.248) \bullet (0.250) + (0.252) \bullet (0.253) = 0.126$, or 12.6% of the time. For a threshold of 0.2 °C, this rises to 16.1%. Hence, dipole configurations are no more ubiquitous than expected by chance. This does not surprise us because TNA and TSA are stochastically independent, i.e., the contingency analysis is consistent with the correlation and goodness-of-fit calculations.

We next consider the occurrence frequency for configurations in which either TNA or TSA, but not both, are anomalous (above or below threshold). We take this condition to be indicative of the occurrence of significant cross-equatorial SSTA gradients given that the tropical Atlantic is not configured as a dipole. This frequency is the sum of the extreme compass point (north, south, east, west) cells of Table 1, or 0.117 + 0.126 + 0.121 + 0.125 = 0.489. For a

threshold of Tq = 0.2 °C we get a frequency of 0.465. Significant meridional gradients, in the absence of dipoles, occur almost half of the time and may be considered three times as common as dipole configurations.

There remains the question of whether these statistics will change appreciably if the meridionally symmetric ENSO variability is first removed from the data, as in the previous section. We therefore repeated this analysis for the (rotated mode) indices NA and SA. Their standard deviations are 0.27 °C and 0.25 °C, respectively and the inter-quartile threshold is Tq = 0.17 °C. Dipole configurations occur 12.7% of the time as compared to an expectation of 12.8%, and significant (non-dipole) gradients occur 47.2% of the time. Although NA and SA are uncorrelated (r=.019), they are not stochastically independent to the same level of confidence as TNA and TSA, because their normality can not be established (p-values<.01). However, the results are nevertheless consistent and suggest no masking effects from the ENSO variability.

5. Correlation and cross-spectral tests

Neither the REOF analysis nor the probability analysis breaks down relationships (or lack thereof) in terms of season or frequency and the former is based on smoothed data sets without intraseasonal variability. Intraseasonal dipole variability, not treated in the REOF analysis of the smoothed K98 data, might be seasonally stronger than the relationship seen in Fig. 1. At interannual and lower frequencies, dipole behavior might be masked, e.g., in seasons when wind speeds are low and shallow mixed layers form. To treat these other aspects we performed crosscorrelation and cross-spectral analyses of the TNA and TSA area indices of the unsmoothed (detrended) K98 data. The analyses were partitioned by calendar month for the correlation analysis and by contrasting seasons for the cross-spectral analysis, over the entire 136-year period (1856-1991). To test for

nonstationarities we performed the same tests on four (4) non-overlapping 34-year data segments.

In Fig. 2 we show the contemporaneous correlation between TNA and TSA by month for the 136-year record. We also show the same result when SSTA in the South Atlantic is averaged only over the 10° square (TSA-2) that produces marginally significant correlations with the NA reconstruction in the REOF analysis (dashed contour in Fig. 1, left panel). For the full TSA index (solid curve) correlations are positive and just below 90% significance during the boreal summer-fall months and near zero at other times. For the more restricted area in the South Atlantic the entire curve is shifted toward negative values and marginally significant (90-95%) negative correlations occur in the boreal winter-spring months (dashed curve). The largest correlations for both curves do not exceed 0.2. When the calculations are repeated for the four 34-year time segments (not shown) the TSA-2 correlation curves consistently shift toward negative values as in Fig. 2 but do not exceed 95% significance, while the seasons of largest positive or negative correlations change randomly. Hence, the overall lack of correlation seen in Fig. 2 is a robust result for the entire 136-year period. Because the correlations are low, do not exceed 95% significance, and do not exhibit a consistent seasonal behavior, we conclude that these tests also fail to reject the null hypothesis of non-dipole behavior.

We performed two other tests with seasonal correlations. We repeated the above calculations using the unsmoothed, detrended K98 data with ENSO removed. The differences were small and did not affect the conclusions. We also calculated correlations for a high-pass filtered version of the data (periods of 1.5 years or longer eliminated) to see if dipole behavior is more evident for purely intraseasonal variability. Any tendency toward antisymmetry is reduced rather than enhanced.

In a final analysis we compute the cross-spectra of TNA vs. TSA (or TNA vs. TSA-2) based on the unsmoothed, detrended K98 data, with and without the global ENSO variability removed. The cross-spectra are computed by a classical Fourier transform method using a Tukey lag window resulting in spectral bands with 12 degrees of freedom and a resolution frequency of 60^{-1} $year^{-1}$. Fig. 3 shows the autospectra, coherence-squared spectra, and phase spectra of the basin-scale indices (TNA, TSA) for both data sets with all seasons included. For added clarity, the phases corresponding to frequencies with insignificant coherence are not shown. As anticipated, there is little reduction in the power spectra of the non-ENSO residuals (dashed) except in the typical ENSO band (3-7 years), and only for TNA. The lack of a similar reduction for TSA is consistent with observations of a stronger ENSO connection in the North Atlantic [*Enfield and Mayer*, 1997]. Both regions show large peaks in the 10-12 year band, but only the TNA energy continues to rise in the multidecadal band (40-60 years).

With ENSO variability included (solid curves) the coherence is highly significant in a band around 2.7 years and is also significant at the lowest frequency (60^{-1} $year^{-1}$). Both bands are more consistent with an in-phase (non-dipole) relationship. Marginally significant coherence, with dipole-consistent phase, occurs near the 12-year periodicity. Removal of the ENSO signal (dashed curves) results in a reduced but still significant coherence of the in-phase variability at 2.7 years, and in the appearance of new coherence peaks (dipole phase) in the 2.3-year and 4.7-year bands. This shows that the presence of ENSO variability can indeed mask tendencies toward a dipole relationship in basin-scale SSTA. This only affects certain interannual frequencies and cannot be detected by an all-spectrum analysis (e.g., the correlations above, or the probability analysis of section 4).

Similar cross-spectral analyses were performed on area indices averaged over two five-month seasons: January through May (JFMAM) and July through November (JASON). These were computed for data with and

without ENSO removed, and for TNA vs. both the basin-scale TSA and the reduced-scale TSA-2 indices. The seasons were chosen based on the time of year when the tropical Atlantic has its greatest (smallest) autospectral energy at low frequencies: JFMAM (JASON). As expected, dipole tendencies are enhanced when ENSO is removed and when the reduced-area index is used. We therefore show only the results for TNA vs. TSA-2 using the non-ENSO residuals (Fig. 4).

The seasonal analyses isolate the following bands of coherence with dipole-consistent phase: 8-12 years and 2.4 years for JFMAM, and 2.3 years and 4.7 years for JASON. The 2.3 and 8-12 year peaks are broader and more significant than the others; the two secondary peaks have only marginal significance in a single frequency band. All of these coherence peaks are related to significant or marginally significant coherence peaks seen in the all-season analysis (Fig. 3). The strong in-phase coherence at 2.7 years (Fig. 3) is absent but appears again in seasonal analyses with the basin-scale TSA index (not shown). It is associated with areas of the South Atlantic other than the TSA-2 region.

6. Summary and discussion

This study has failed to find significant basin-scale dipole variability in tropical Atlantic SSTA, except for certain spectral bands when area indices are averaged for the boreal winter-spring or summer-fall season and/or ENSO is removed. Otherwise, dipole configurations at basin-scale occur infrequently and only with chance expectation. We find only one indication of a possible antisymmetric SSTA relationship across the ITCZ: there is a weak tendency for SSTA over a small region west of Angola to be of opposite sign to basin-scale SSTA departures in the tropical North Atlantic (Fig. 1, left). The opposite is not true for any areas in the tropical North Atlantic with respect to basin-scale fluctuations in the South Atlantic. The seasonally stratified spectral analysis indicates that a dipole relationship does occur in two period bands: 8-

12 years (boreal winter-spring) and 2.3 years (summer-fall). It is possible in these instances that dipole configurations are excited by a stronger meridional gradient mode, such as the mode suggested by *Chang et al*. [1996]. However, the amount of full-spectrum, local variance explained in the South Atlantic by correlation with basin-scale fluctuations in the North Atlantic does not exceed 7% even in the regionally sensitive area west of Angola. Hence, any intrinsic dipole variability is not a dominant feature of tropical Atlantic SSTA.

The lack of a dominant dipole mode of SSTA variability does not mean that significant fluctuations in meridional SSTA gradients do not occur, nor that such fluctuations are unimportant for the climate of the tropical Atlantic and surrounding land regions [e.g., *Huang et al.*, 1995; *Wagner*, 1996; *Carton et al.*, 1996]. Quite to the contrary, our analysis shows that non-dipole configurations associated with significant meridional SSTA gradients are common, they occur nearly half of the time. In fact, an index based on the difference between TNA and TSA, as suggested by *Servain* [1991], is really quite useful for Atlantic climate analysis precisely because it indexes the meridional SSTA gradient. Significant non-zero values of the index need not and usually do not result from dipole configurations, even though pointwise correlation of the index with SSTA produces a dipole pattern. Therefore, to call the index a "dipole index" is misleading.

Because dipole configurations (which occur only with chance frequency) are associated with the largest SSTA gradients, analyses such as gridded SSTA correlated against rainfall indices will typically indicate a dipole distribution for associated SSTA, since that is the optimal configuration for anomalous rainfall. The pointwise correlation pattern of SSTA with TNA-TSA is a case in point. In general, dipole distributions of SSTA emerge in analyses organized around the bivariate relationships of SSTA with anomalies of atmospheric variables that are sensitive to ITCZ latitude and meridional SSTA gradient (e.g., rainfall, wind, or SLP). Such analyses are evidence that

gradient-climate covariability is real. They do not mean that dipole configurations of SSTA occur as part of an intrinsic interaction, nor do they imply that they are a dominant mode of variability, intrinsic or otherwise. Misinterpretation of such patterns, with direct or implied references to a dipole mode, can potentially pose the wrong questions for future research.

The Pilot Research Moored Array in the Tropical Atlantic (PIRATA) being implemented by Brazil, France and the United States [*Servain et al*., 1998] is shown superimposed on the REOF distributions of Fig. 1. The array appears to be well positioned to effectively sample the SSTA variabilities in the regions of high explained variance on either side of the ITCZ. One of the future challenges for empirical analyses of the data and for modeling studies will be to show why plausible ocean-atmosphere feedback mechanisms, such as proposed by *Chang et al*. [1997], explain observed relationships involving the meridional SSTA gradient yet do not lead to more frequent occurrences of dipole configurations or greater cross-equatorial coherence. What are the large-scale climate processes, such as the North Atlantic Oscillation (NAO) that separately control the variability of SSTA in the TNA and TSA regions? How are these processes related to each other, and why do they result in uncorrelated fluctuations on opposite sides of the ITCZ? We should not be asking how dipole variability can be produced. The more significant query is: why do the North and South Atlantic fluctuate as independently as they do?

Acknowledgments. J. Harris prepared all of the basic data sets used in this project. This work has been supported by base funding from the Environmental Research Laboratories, by a grant from the Pan-American Climate Studies program, by a grant from the Inter-American Institute for Global Change Research (IAI), and by FONDECYT grant No 1980117.

References

Bartoszynski R., M. Niewiadomska-Bugaj, *Probability and Statistical Inference*, Wiley and Sons, New York, 1996.

Bottomley, M., C.K. Folland, J. Hsiung, R.E. Newell, and D.E. Parker, *Global Ocean Surface Temperature Atlas*, Her Majesty's Stn. Off., Norwich, England, 1990.

Carton, J.A., X. Cao, B.S. Giese, and A.M. da Silva, Decadal and interannual SST variability in the tropical Atlantic Ocean, *J. Phys. Oceanogr., 26*, 1165-1175, 1996.

Chang. P., L. Ji, and H. Li. A decadal climate variation in the tropical Atlantic Ocean from thermodynamic air-sea interactions, *Nature, 385*, 516-518, 1997.

Davis, R.E. Predictability of sea surface temperature and sea level pressure anomalies over the North Pacific Ocean, *J. Phys. Oceanogr., 6*, 249-266, 1976.

Enfield, D.B. Relationships of inter-American rainfall to tropical Atlantic and Pacific SST variability, *Geophys. Res. Lett.*, *23*, 3305-3308, 1996.

Enfield, D.B. and D.A. Mayer. Tropical Atlantic SST variability and its relation to El Niño-Southern Oscillation, *J. Geophys. Res.*, *102*, 929-945, 1997.

Enfield, D.B. and A.M. Mestas-Nuñez, Multiscale variabilities in global sea surface temperatures and their relationships with tropospheric climate patterns, *J. Climate,* 1998 (in press).

Folland, C.K., T.N. Palmer and D.E. Parker, Sahel rainfall and worldwide sea temperatures, *Nature, 320*, 602-607, 1986.

Hastenrath, S. Variations in low-latitude circulation and extreme climatic events in the tropical Americas, *J. Atmos. Sci., 33*, 202-215, 1976.

Hastenrath, S. and L. Greischar, Circulation mechanisms related to northeast Brazil rainfall anomalies, *J. Geophys. Res., 98*, 5093-5102, 1993.

Hogg, R.V., and A.T. Craig, *Introduction to Mathematical Statistics*, The Macmillan Company, New York, 383 pp., 1965.

Houghton, R.W. and Y.M. Tourre, Characteristics of low-frequency sea surface temperature fluctuations in the tropical Atlantic, *J. of Clim., 5*, 765-771, 1992.

Huang, B., J.A. Carton, and J. Shukla, A numerical simulation of the variability in the tropical Atlantic Ocean, 1980-88, *J. Phys. Oceanogr., 25*, 835-854, 1995.

Kaplan, A., M.A. Cane, Y. Kushnir, A.C. Clement, M.B. Blumenthal, and B. Rajagopalan, Analysis of Global Sea Surface Temperatures 1856-1991, *J. Geophys. Res., 103*, 18,567-18,589, 1998.

Lamb, P.J., and R.A. Peppler, Further case studies of tropical Atlantic surface atmospheric and oceanic patterns associated with sub-Saharan drought, *J. of Clim., 5*, 476-488, 1992.

Mehta, V.M., Variability of the tropical ocean surface temperatures at decadal-multidecadal timescales. Part I: The Atlantic Ocean, *J. of Clim., 11*, 2351-2375, 1998.

Mehta, V.M. and T. Delworth, Decadal variability of the tropical Atlantic Ocean surface temperature in shipboard measurements and in a global ocean-atmosphere model, *J. of Clim., 8*, 172-190, 1995.

Mestas-Nuñez, A.M. and D.B. Enfield, Rotated global modes of non-ENSO sea surface temperature variability *J. Climate.*, 1998, (submitted).

Moura, A.D. and J. Shukla. On the dynamics of droughts in northeast Brazil: Observations, theory and numerical experiments with a general circulation model, *J. Atmos. Sci., 38*, 2653-2675, 1981.

Nobre, P. and J. Shukla, Variations of sea surface temperature, wind stress, and rainfall over the tropical Atlantic and South America, *J. of Clim., 9*, 2464-2479, 1996.

Rajagopalan, B., Y. Kushnir, and Y.M. Tourre, Observed decadal mid-latitude and tropical Atlantic climate variability, *Geophys. Res. Lett.*, *25*, 367-370.

Servain, J. Simple climatic indices for the tropical Atlantic Ocean and some applications, *J. Geophys. Res., 103*, 15,137-15,146, 1991.

Servain, J., A.J. Busalacchi, M.J. McPhaden, A.D. Moura, G. Reverdin, M. Vianna, and S.E. Zebiak, A Pilot Research Moored Array in the Tropical Atlantic, *Bull. Am. Met. Soc.*, *79*, 2019-2031, 1998.

Shriver, J.F. and J.J. O'Brien, Low-frequency variability of the equatorial Pacific Ocean using a new psuedostress dataset: 1930-1989, *J. Clim.*, *8*, 2762-2786, 1995.

Smith, T. M., R. W. Reynolds, R. E. Livezey, and D.C. Stokes, Reconstruction of historical sea surface temperatures using empirical orthogonal functions. *J. Clim, 9*, 1403-1420, 1996.

Wagner, R.G., Mechanisms controlling variability of the interhemispheric sea surface temperature gradient in the tropical Atlantic, *J. Climate, 9*, 2010-2019, 1996.

Weare, B.C., Empirical orthogonal function analysis of Atlantic Ocean surface temperatures, *Quart. J. Roy. Met. Soc., 103*, 467-478, 1977.

Table 1. Contingency table of frequencies (fraction of 1.0, shown in italics within the bordered cells) for which TNA or TSA values fall in their extreme quartile ranges, or in a bi-quartile mid-range. The row and column sums (referred to in the text) are shown outside of the bordered matrix.

	TNA≥Tq	**|TNA|<Tq**	**TNA≤-Tq**	**TOTAL**
TSA≥Tq	***0.069***	***0.117***	***0.062***	**0.248**
|TSA|<Tq	***0.125***	***0.254***	***0.121***	**0.500**
TSA≤-Tq	***0.059***	***0.126***	***0.067***	**0.252**
TOTAL	**0.253**	**0.497**	**0.250**	**1.000**

Figure Captions:

Figure 1. Upper panels: tropical Atlantic distributions of correlation between the gridded *Kaplan et al*. [1998] SSTA data (smoothed, ENSO and trends removed) and two rotated EOFs of the data with high explained variance in the North (NA, left) and South Atlantic (SA, right). Positive values are shaded with solid contours, negative contours are dashed, the heaviest contour is zero, and the contour interval is 0.2. Dashed rectangles denote the areas over which the TNA and TSA area indices of SSTA are calculated. Small circles show the mooring positions for the proposed PIRATA array [*Servain et al*., 1998]. Lower panels: temporal reconstructions of the NA, SA modal contributions to the SSTA variability within the respective TNA and TSA index areas.

Figure 2. Solid curve: correlation, partitioned by calendar month, between the TNA and TSA indices of SSTA computed from unsmoothed and detrended K98 data (solid curve). Dashed curve: as for the solid curve, but for TNA versus SSTA averaged over a 10°x10° region west of Angola (TSA-2) that approximates the dashed contour in Fig. 1 (upper left panel). Gray shading (horizontal dashed lines) outlines values below 90% (95%) significance

Figure 3. First and second panels: autospectra for the TNA and TSA area indices based on the unsmoothed and detrended K98 data (solid), and based on the same data with the global ENSO mode removed (dashed). Third panel: as above but for the coherence-squared spectra. The 90%-95% significance range is shaded in gray. Fourth panel: estimates of spectral phase in bands where the coherence-squared is significant at the 90% level or higher. Solid (unfilled) circles correspond to solid (dashed) coherence-squared curve. Phase regions within 45° of zero and ±180° are shaded.

Figure 4. As in Figure 3, for the unsmoothed K98 data with trends and ENSO removed, except: a) the indices compared are TNA and TSA-2; and b) the solid (dashed) curves refer to seasonal averages for the boreal winter-spring (summer-fall) season.

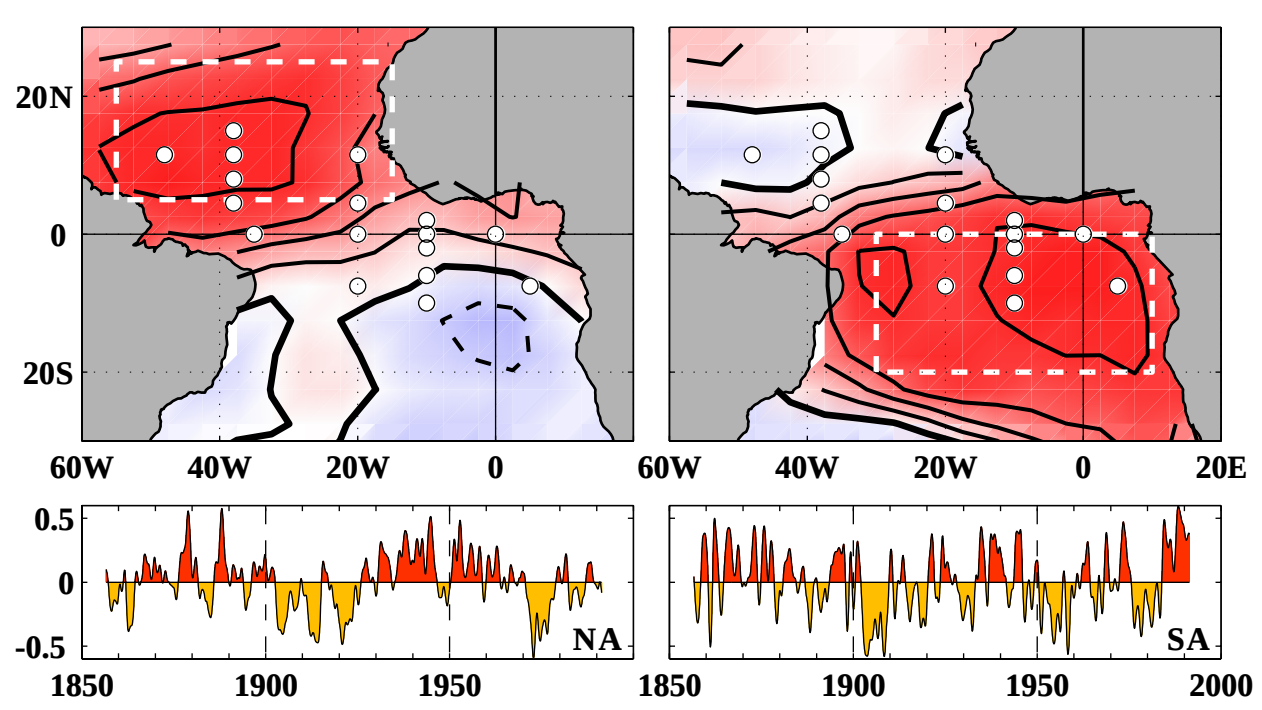
20N
0
20S
60W
40W
20W
0
60W
40W
20W
0
20E
0.5
0
-0.5
NA
SA
1850
1900
1950
1850
1900
1950
2000

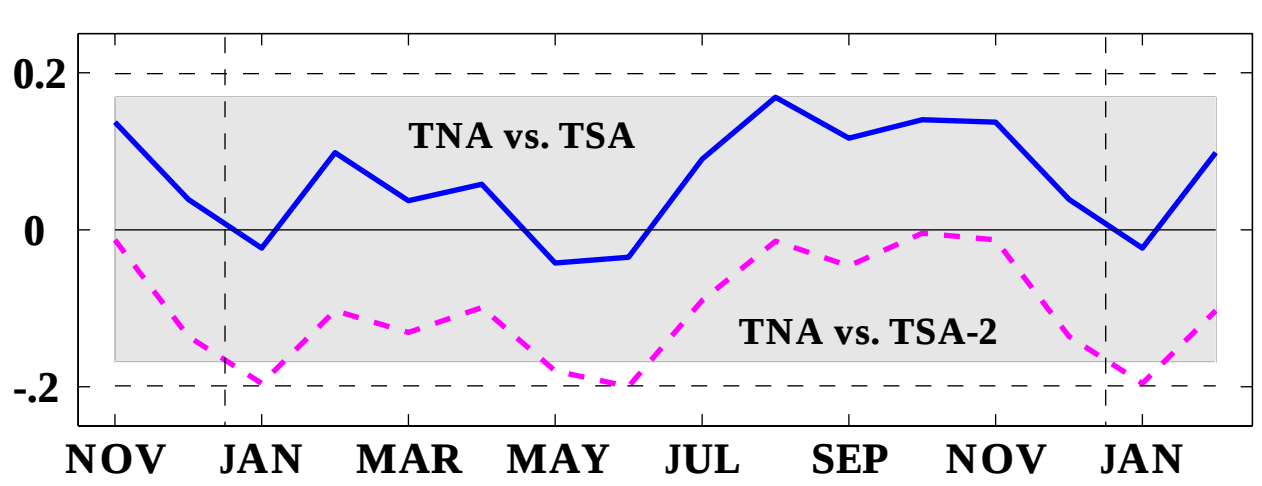
0.2
0
-.2
TNA vs. TSA
TNA vs. TSA-2
NOV
JAN
MAR
MAY
JUL
SEP
NOV
JAN

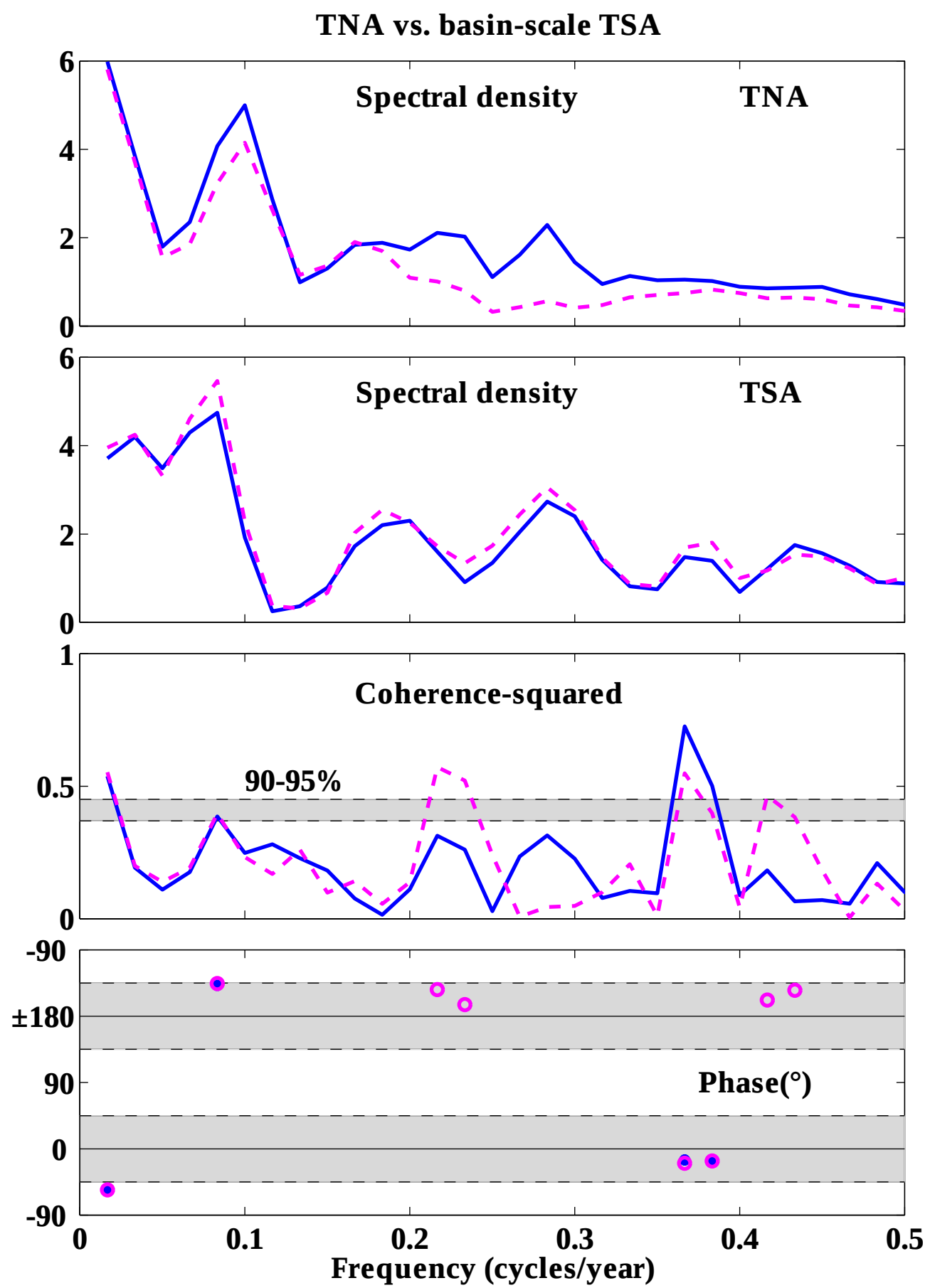
TNA vs. basin-scale TSA
Spectral density
TNA
Spectral density
TSA
Coherence-squared
90-95%
Phase(°)
6
4
2
0
1
0.5
-90
±180
90
0
0.1
0.2
0.3
0.4
0.5
Frequency (cycles/year)

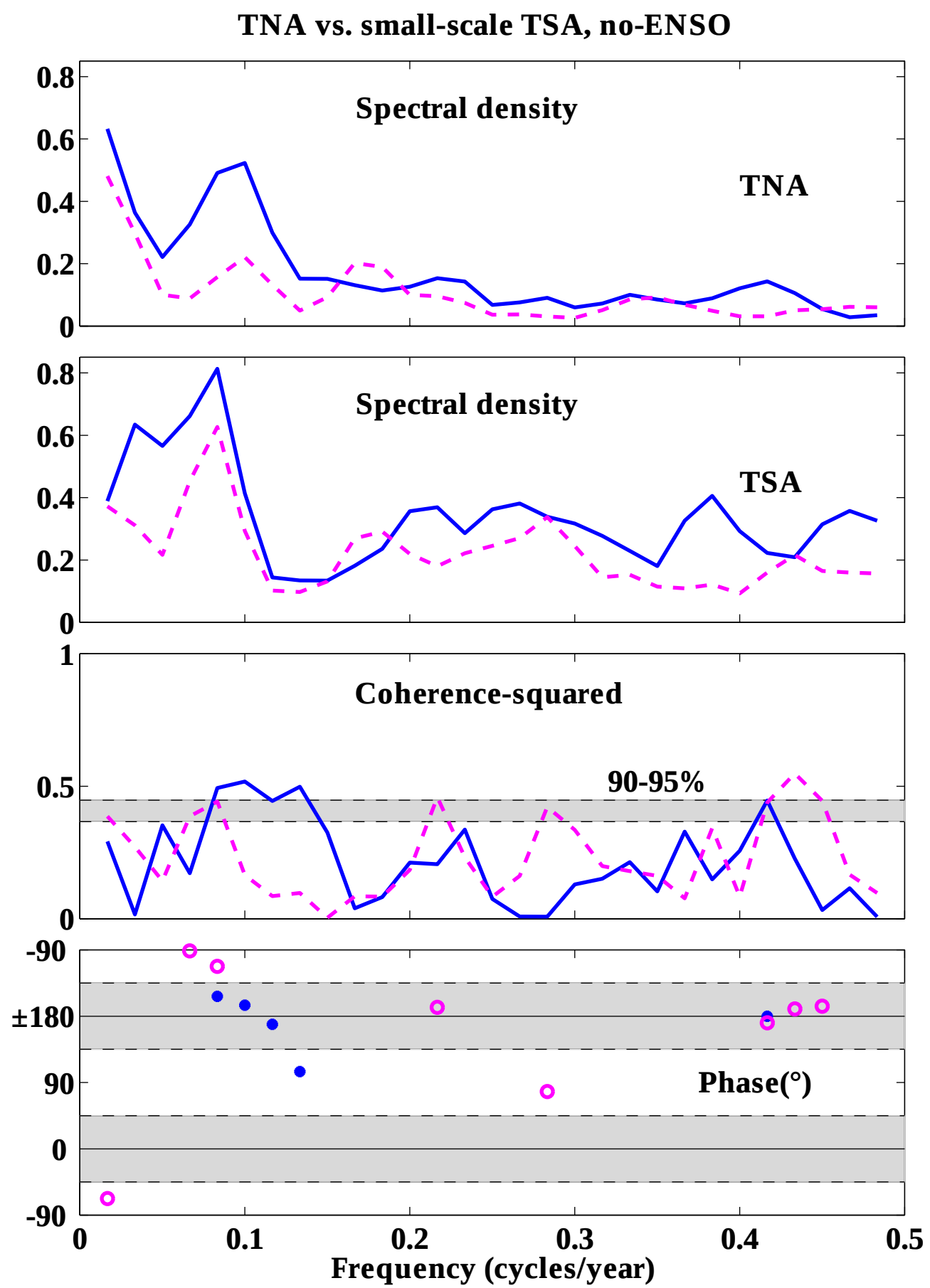
TNA vs. small-scale TSA, no-ENSO
Spectral density
TNA
0.8
0.6
0.4
0.2
0
Spectral density
TSA
0.8
0.6
0.4
0.2
0
Coherence-squared
90-95%
1
0.5
0
-90
±180
90
0
-90
Phase(°)
0
0.1
0.2
0.3
0.4
0.5
Frequency (cycles/year)